INTERACTIVE CONTROL ENGINEERING
Principles and Applications

Volume 3 Feedforward, Cascade, and Ratio Control

CHAPTER 12

Gravity Feedforward and Input Shaping for a Speculative Space Elevator Climber

Pages 286–312

Edited by John D. Hedengren

How to cite this chapter. "Gravity Feedforward and Input Shaping for a Speculative Space Elevator Climber," in *Feedforward, Cascade, and Ratio Control*, John D. Hedengren, Ed., vol. 3 of *Interactive Control Engineering: Principles and Applications*. Advanced Process Solutions, LLC, 2026, ch. 12, pp. 286–312.

The page numbers in this file are those of the printed volume.

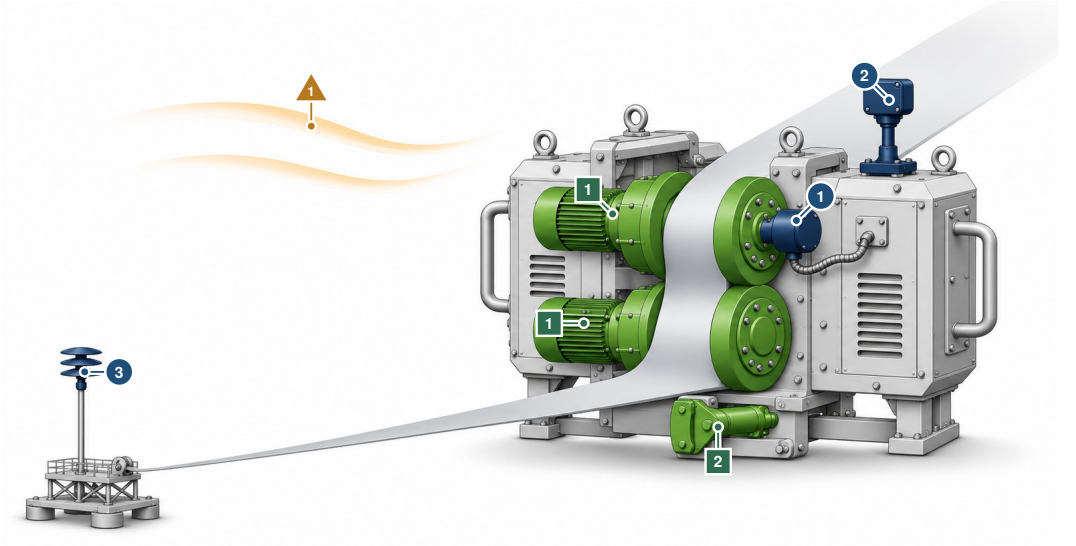
The app for this chapter
https://apmonitor.com/apps/space-elevator/

The volume online: contents, other chapters and citation records
https://apmonitor.com/apps/books/v03-feedforward-cascade/#space-elevator

Copyright © 2026 Advanced Process Solutions, LLC. All rights reserved. Produced by Advanced Process Solutions, LLC.

CHAPTER 12

Gravity Feedforward and Input Shaping for a Speculative Space Elevator Climber



The controller moves 1 motors that drive the rollers 2 friction brake

The controller reads 1 roller speed 2 height, by ranging 3 wind report from a profiler

What disturbs it 1 crosswind and gusts

Notice that the climber hangs on a long, slowly swaying ribbon, so every change of its speed and every gust of crosswind pushes it sideways. Illustration, not to scale.

IN PLAIN TERMS Climbing a Ribbon Into Space

The main idea. A space elevator would be a very long ribbon hanging down from high above the Earth. A machine would climb it on motor-driven rollers, and its controller is told in advance how its weight shrinks with height.

The challenge. Each time the climber speeds up or slows down, the turning Earth pushes it sideways and the ribbon swings slowly. Wind, motor heat and the power supply also limit how fast it may climb.

Why it matters. No such elevator has been built, but planning a move on a long, swaying cable matters for cranes and mine hoists too.

THREE WAYS TO READ THIS CHAPTER

Explore	13 min	the first page, the fact on the ribbon's length (Section 12.1), the two history segments (Section 12.2), the two try-it segments and the fact on the descent (Section 12.6) and the key points
Study	50 min	the whole chapter with its three pause points and the twelve exercises at its end
Practice	20 min	the first page, the results (Section 12.6), Technology in Practice (Section 12.7), Limitations (Section 12.8) and the two open challenges

The control question A climber on a space elevator ribbon carries a weight that falls from 9.76 m/s^2 at the anchor to zero at the geostationary radius, and every change of its speed pushes the ribbon sideways through the Coriolis force. What do a gravity feedforward, a speed schedule, an input shaper and a feasibility supervisor each contribute when the load, the structure and the limits all change along the route?

Learning objectives

- Compute the effective gravity, the geostationary radius and the error of a constant-gravity feedforward at any height on the route.
- Estimate the period and damping of the climber's local mode from the string below it and the impedance of the ribbon above.
- Design ZV and ZVD shapers from a predicted mode and explain why they remove the ringing after a move but not the lag during it.
- Explain why a speed schedule slows the climber in a crosswind and on a descent, and read the price in trip time.
- Combine schedule, shaper and feedforward to pass the graded transfer inside every limit.

Prerequisites Sections 1.4.2 (where a disturbance enters), 1.4.3 (static feedforward), 1.6.2 (velocity form) and 1.6.4 (scenarios and the challenge). Chapter 10 for a gravity feedforward on a vehicle and Chapter 11 for motion in a rotating frame.

The app https://apmonitor.com/apps/space-elevator/

See also Volume 7, Chapter 12 for ZV and ZVD shapers on a swinging load with an assumed cable length, and Volume 20, Chapter 3 and Volume 20, Chapter 4 for load-sheet feedforward and supervised flight on vehicles whose load and authority change along the route.

12.1 Introduction

Every hoist in ordinary service carries a load whose weight does not change on the way up. An elevator car, a crane hook and a mine skip weigh the same at the top of their travel as at the bottom, and what changes with the operating point is the rope. A deep mine hoisting cable changes length as the conveyance travels, and its coupled lateral and longitudinal response is governed by equations that accommodate that non-stationary nature [1]. Command shaping grew up around flexible systems of this kind, where a commanded move excites a lightly damped mode that rings long after the move ends [2–4], and high-performance motion control pairs a trajectory with bounded derivatives with a feedforward matched to it [5].

A space elevator would reverse that arrangement. A climber rides a ribbon from an anchor on the equator through the geostationary radius to a counterweight beyond it [6–8], and in the frame that turns with the Earth its weight is set by the effective gravity $\mu/r^2 - \omega^2 r$. On the ribbon simulated here that is 9.764 m/s^2 at the anchor, 9.318 m/s^2 at the 150 km station and zero at 42 164 km from the Earth's center, so the drive force that holds an 11 t climber still falls from 107.4 kN to nothing over the route. The ribbon is a string whose slowest lateral mode has a period of 127.4 h. A climber moving outward at speed v is pushed west by the Coriolis force $2m\omega v$, only 80.2 N for 11 t at 50 m/s. Its guide rollers pass that push to the ribbon, whose primary response to an ascending climber is a rotation opposite to the Earth's rotation [9]. Every change of the climber's speed changes that push.

> ✦ DID YOU KNOW? **Three Weeks End to End**
>
> A NASA-sponsored study pictured an elevator ribbon several meters wide, thinner than a piece of paper and about 100 000 km long. Climbers splicing new ribbon onto it at 200 km per hour would each need 21 days to travel its full length [10].

The concept is speculative, and the application treats it that way. The orbital tower had to overcome buckling, strength and dynamic stability, and its strength problem was answered on paper by an

exponential taper [7]. The strength of a real carbon nanotube cable, with the defects a cable of that length cannot avoid, has been estimated at least about 70 % below the theoretical strength of the nanotubes, enough to cast doubt on the construction [11], and powering the climbers and surviving micrometeoroids, lightning and debris are problems as important as producing the cable [8]. The simulator gives its ribbon a working specific strength of 40 MJ/kg, more than eleven times the 3.5 MJ/kg its parameter panel quotes for carbon fiber, and it takes the 6 MW power supply, the guideway and the anchor platform as declared inputs. It demonstrates numerical convergence and reduced-order plausibility. It does not show that an Earth space elevator can be built, and none of its numbers are those of a real one.

The plant corrects two beliefs that a transfer function leaves intact. The first is that a vehicle's weight is a constant that a controller can be tuned around once. A feedforward of the constant $g_0 = 9.806\,65\,\mathrm{m/s^2}$ is 0.43 % high at the anchor and 5.2 % high at 150 km, while 34 km past the geostationary altitude it believes in a 107.9 kN weight that is not there and throws the climber outward to 169.1 m/s. The second is that a structure too slow to matter to the drive can be left out of the command. The climber's local mode, its own mass on the ribbon below it, has a period of 8.9 min at 150 km, and a departure that reaches cruising speed in 4 min leaves the climber 30.8 m behind its moving lean and then 21.4 m past it. The same shape, a moving load on a long and lightly damped structure, appears in hoisting cables of changing length [1], in cranes and flexible manipulators [4] and in the elevator ribbon itself [12, 13]. However, dynamics studies of the elevator have treated the climber's motion as a prescribed transit [9] or as the decision variable of an optimization of the residual libration [13], while the motion a real climber can make is also bounded by its drive, its supply, the heat of its motor, its brakes and the air, and has to be flown by feedback on measurements.

This chapter measures what a gravity feedforward, a speed schedule, an input shaper and a feasibility supervisor are each worth on a speculative space elevator climber simulator. Each of these methods, and the elevator concept itself, is established. Section 12.2 reviews the concept, the dynamics of its ribbon and the history of shaped commands. Section 12.3 sets out the model with every relation and constant: a reduced-order ribbon of six finite-element modes, a residual-flexibility local mode that carries the climber's mass, and an energy ledger that closes to 3.8×10^{-10} of the energy through it on the scheduled descent. Section 12.4 examines the effective gravity along the route and approximates the climber's local mode as its own mass on the string below it, with the ribbon above acting as a dashpot of coefficient T/c. The approximation reproduces the application's periods to within 2.7 % up to 150 km and explains why the mode is lightly damped near the anchor and well damped high up. Section 12.5 gives the five layers of the controller, and Section 12.6 reports eight focused cases and a graded transfer, in which each control layer can be removed and its cost read off the scorecard. Section 12.7 sets the loops on the hardware a climber would carry, Section 12.8 states the limitations, Section 12.9 sums up, and the exercises of Section 12.10 run the cases again.

12.2 Elevator Concepts, Ribbon Dynamics and Shaped Motion

The idea of a structure reaching from the ground past the geostationary orbit is more than a century old, and it received serious scientific attention only after carbon nanotubes were discovered [14]. A letter of 1966 examined self-supporting cables extending into space from the Earth and from other rotating or revolving bodies, and observed that masses could in principle be launched with energy drawn entirely from the rotation of the central body [6]. The orbital tower of 1975 connected a geostationary satellite to the ground, named buckling, strength and dynamic stability as the three problems it had to overcome, and solved the strength problem with a cross-section tapered exponentially with the gravitational and inertial forces, largest at the geostationary point [7]. That taper is the constant-stress ribbon of Section 12.3.

The first studies concluded that no material then available had the required properties. After carbon nanotubes appeared in 1991, a design and deployment study returned to the construction and listed the powering of the climbers and the survival of micrometeoroid impacts, lightning strikes and

debris collisions among the problems to solve [8]. A study commissioned by NASA in the late 1990s examined the feasibility of such a structure and its applications [14]. Models of a real, and therefore defective, nanotube cable some 100 Mm long then placed its strength at least about 70 % below the theoretical nanotube strength, a reduction that puts the realization of the elevator in doubt [11].

> ⧖ **HISTORY** **A NASA Workshop Weighs the Elevator, 1999**
>
> A workshop held at a NASA flight center in 1999 asked whether the space elevator could be a possible future project instead of pure science fiction. Its findings were cautious. The materials the structure needed were still in laboratory development, and an elevator from the Earth to the geostationary orbit was judged not feasible at the time, though it might become possible in the latter part of the twenty-first century. A tether hanging down from the geostationary orbit to a tall tower built up from the ground appeared the most efficient and feasible form. The workshop's vehicle rode its track by electromagnetic propulsion, because traction wheels would be much slower and would wear both the vehicle and the structure [15]. The climber of this chapter takes the other path, rollers clamped on a ribbon.

Space tether research has its own review literature [16]. The elastic oscillations of the elevator ribbon have been modeled with assumed modes for its longitudinal extension and its transverse motion about a librating reference line [12]. A planar model of climber transit showed that the ribbon's primary response to an ascending climber is a westward rotation produced by the Coriolis force on the moving climber [9], and the climber's motion along the tether has been chosen by dynamic optimization to minimize the residual in-plane libration of the ribbon and the counterweight [13]. The industrial relatives are older. Deep mine hoisting cables have been modeled as a distributed-parameter system whose lateral and longitudinal oscillations interact through quadratic and cubic terms while the cable length changes [1].

> ⧖ HISTORY **A Tether Deployed to a Planned Profile, 1993 and 1994**
>
> Two small experiments, flown as secondary payloads in 1993 and 1994, each unreeled a tether of 20 km from a rocket stage. The first deployed it open loop. At the end of the deployment its tether was still running out at about 7 m/s, which the handbook of the field gives as the reason for a huge jump in tension and the rebounds that followed. The second flight closed the loop on a profile computed before the mission. Its control logic acted on a friction brake, speeding the deployment up or slowing it down to follow the profile and bring the payload to a smooth stop along the local vertical. The final tether rate was about 2 cm/s and the final libration about 4 degrees [17]. A planned trajectory with feedback around it is also the pairing of the climber's planner and speed loop.

Shaping a command against a structural mode began with Posicast control, which excites several transient oscillations at closely spaced times, with magnitudes and phases chosen so that their phasors sum to zero, and gives a half-cycle response when a step is split into two spaced excitations [2]. Preshaped commands that stay robust under parameter uncertainty cost a move-time penalty of about one period of the first mode and cut the endpoint residual vibration of a Space Shuttle Remote Manipulator System simulator by a factor of 25 [3]. The first fifty years of command shaping for flexible systems have been reviewed [4], and Volume 7, Chapter 12 applies the same shapers to the swinging load of a gantry crane, with timings taken from an assumed cable length. In high-performance motion systems the command is itself a point-to-point trajectory with bounds on its derivatives, time-optimal in the most relevant cases, fed forward through a controller of matching order [5]. The simulator combines all three, a bounded-jerk trajectory, a shaper and a model feedforward, on a plant whose load and whose mode both change with height.

12.3 Climber, Ribbon and Loads

The simulated system is a climber of mass m on a ribbon anchored at the equator, described in the frame that turns with the Earth. Heights $z = r - R_E$ are measured outward from the anchor and lateral displacements eastward in the orbit plane. The route, the climber, its forces, its local link to the ribbon and its instruments are shown in Figure 12.1. Thirty states are integrated together, namely the height, the speed and the developed drive force, the motor and brake temperatures, eight modal coordinates and their rates of which six are used, the climber's lateral position and velocity, and seven energy ledgers. Table 12.1 lists the variables by role.

12.3.1 Effective Gravity and the Declared Ribbon

A point held on the ribbon at radius r feels gravity inward and the effect of turning with the Earth outward. Their difference is the effective gravity of Equation (12.1), the radial derivative of the effective potential Φ.

$$g_{eff}(r) = \frac{\mu}{r^2} - \omega^2 r = \frac{\mathrm{d}\Phi}{\mathrm{d}r}, \qquad \Phi(r) = -\frac{\mu}{r} - \frac{\omega^2 r^2}{2} \tag{12.1}$$

Here μ is the Earth's gravitational parameter and ω its sidereal rotation rate. The effective gravity vanishes at the geostationary radius $r_{GEO} = (\mu/\omega^2)^{1/3} = 42\,164.17\,\mathrm{km}$, which is 35 786 km above the anchor, and it points outward beyond that radius, reaching $-0.492\,\mathrm{m/s^2}$ at the 100 000 km counterweight.

The ribbon is a hypothetical constant-stress design. Every cross-section works at the same stress σ_w, so its linear density follows its tension, $\lambda = T/c^2$ with $c^2 = \sigma_w/\rho_r$ the working specific strength and ρ_r the material density, and the static balance $\mathrm{d}T/\mathrm{d}r = \lambda g_{eff}$ integrates to Equation (12.2).

$$T(r) = T_0\, \mathrm{e}^{[\Phi(r) - \Phi(R_E)]/c^2}, \qquad M_{cw} = \frac{T(r_{cw})}{\omega^2 r_{cw} - \mu/r_{cw}^2} \tag{12.2}$$

where T_0 is the anchor tension with no climber on the ribbon and M_{cw} is the counterweight that the tension at r_{cw} holds in place. With $c^2 = 40\,\mathrm{MJ/kg}$ and $T_0 = 320\,\mathrm{kN}$ the tension grows to 1073.7 kN

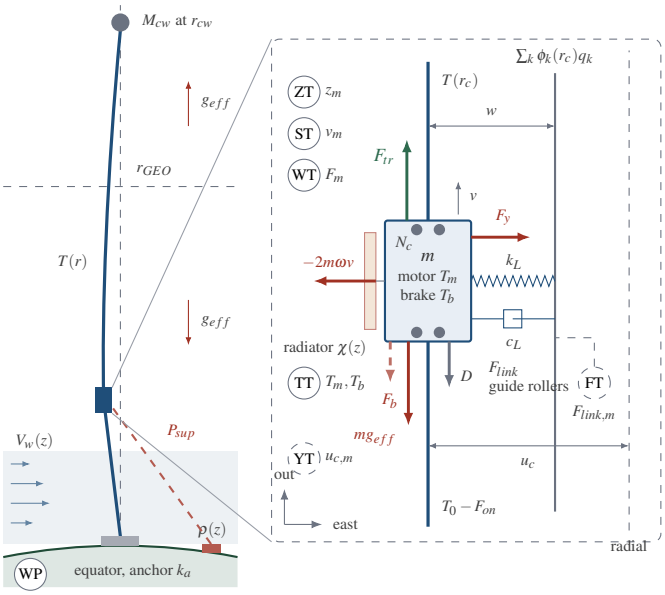


Figure 12.1 Space elevator as modeled, not to scale. Left, the route: the anchor of lateral stiffness k_a, the atmosphere $\rho(z)$ with the crosswind profile $V_w(z)$, the ribbon of tension $T(r)$ leaning west behind a climbing climber, the geostationary radius where g_{eff} changes sign, the counterweight M_{cw} at r_{cw}, the hypothetical power delivery P_{sup} and the wind profiler WP. Right, the climber of mass m on traction rollers clamped with force N_c, with its drive force F_{tr}, brake F_b, drag D, weight mg_{eff}, Coriolis force $-2m\omega v$ and side load F_y, and the local link k_L, c_L that carries F_{link} to the ribbon's modal shape. Solid instruments are read by the controller and dashed ones are only logged.

at the geostationary radius and falls to 712.7 kN at the counterweight, the density rises from 0.0080 to 0.0268 kg/m, and the ribbon weighs 2146.9 t with a 1448.9 t counterweight. The same c, 6325 m/s, is the lateral wave speed everywhere, since $\sqrt{T/\lambda} = c$. These dimensions follow from the declared inputs and are not the result of a design study.

Table 12.1 Climber Variables by Role, With Defaults and Ranges

Symbol	Role, unit	Default	Range
v	CV, speed loop, m/s	$v_{sh}+\Delta v$	$\le v_{lim}(z)$
z	CV, station stop, km	SP 150	0–40 000
F	MV, force demand, kN	MANUAL 0	−400 to 280
$F_{d,cmd}$	allocated motor command, kN	—	±280
$F_{b,cmd}$	allocated brake command, kN	—	0 to $F_{b,cap}$
Δv	MV of the height trim, m/s	0	±2
V_j	DV, crosswind at z_j, m/s	0	±30
σ_g	DV, gust intensity, m/s	0	0–8
p_s	DV, supply asked, %	100	0–100
b_v	DV, tachometer bias, m/s	0	±2
Δm	DV, cargo off the sheet, t	0	−5 to 8
F_{link}	limit, guide rollers, kN	—	≤ 6.00
T_a	limit, anchor tension, kN	320	≥ 64
T_m, T_b	limits, motor, brake, °C	20	≤ 150, ≤ 600
z, v, F_d	states, height, speed, drive	per case	—
T_m, T_b	states, temperatures, K	293.15	—
q_k, $\dot{q}_k$	states, 8 slots, 6 used, m	quasi-static	—
u_c, $\dot{u}_c$	states, climber lateral, m	quasi-static	—
$E_{in}\ldots E_{dmp}$	states, 7 ledgers, J	0	—

12.3.2 The Climber Along the Ribbon

The climber obeys the radial momentum balance of Equation (12.3), with the drive developing its force through a first-order lag.

$$\begin{aligned} m\frac{\mathrm{d}v}{\mathrm{d}t} &= F_{tr}+F_b-m\,g_{eff}(r)-D, \qquad \frac{\mathrm{d}z}{\mathrm{d}t}=v \\ \tau_F\frac{\mathrm{d}F_d}{\mathrm{d}t} &= \mathrm{clamp}(F_{d,cmd},\,\pm F_I)-F_d \\ D &= \tfrac{1}{2}\,\rho(z)\,C_D A_f\,|v|\,v \end{aligned} \tag{12.3}$$

Here F_d is the force the motor has developed, F_I its force at the current limit, $C_D A_f$ the axial drag area and $\rho(z)=\rho_0 \mathrm{e}^{-z/H}$ below 200 km and zero above. The traction force F_{tr} is F_d after the three limits of Equation (12.4).

$$\begin{aligned} |F_{tr}| \le F_P &= \frac{-|v|+\sqrt{v^2+4c_{cu}(P_{av}-P_{aux})}}{2c_{cu}}, \quad F_d v \ge 0 \\ |F_{tr}| \le F_R &= \frac{|v|-\sqrt{v^2-4c_{cu}(P_{aux}+P_{rg})}}{2c_{cu}}, \quad F_d v < 0 \\ P_{el} &= F_{tr}\,v+c_{cu}F_{tr}^2+P_{aux} \end{aligned} \tag{12.4}$$

The first bound keeps the electrical power P_{el} within the power P_{av} the supply delivers, and the second keeps the power returned by regeneration within the P_{rg} the supply accepts, with no bound where the discriminant is not positive because the losses then absorb all of it. The third limit is the grip of the rollers. Above the static traction $\mu_s N_c = 225\,\mathrm{kN}$ they slide and deliver $\mu_k N_c = 175\,\mathrm{kN}$. The available power P_{av} follows the power asked, $P_{sup}\,p_s/100$, at a ramp rate of 25 % of the 6 MW supply per minute.

The friction brake always opposes the motion and fades when hot, as shown in Equation (12.5).

$$\begin{aligned} F_b &= -\min\left[F_{b,cmd},\, F_{b0} f(T_b)\right] \frac{v}{\sqrt{v^2+v_\varepsilon^2}} \\ f &= \max\left[0.4,\; 1-0.6\,(T_b-T_{fade})/200\,\mathrm{K}\right] \end{aligned} \tag{12.5}$$

with $f=1$ below $T_{fade}=650\,^\circ\mathrm{C}$ and $v_\varepsilon=0.05\,\mathrm{m/s}$ smoothing the direction through zero speed. Two contacts hold the climber at rest as hybrid states. On the platform, $z\le 0$, the climber is held while $F_{tr}+F_b-mg_{eff}\le 0$ and $v\le 0$, and a landing faster than 2 m/s is recorded as an impact. The parking clamp engages on command once $|v|\le 0.05\,\mathrm{m/s}$, carries the climber's weight and slips if the net force $|F_{tr}-mg_{eff}|$ exceeds the brake capacity.

12.3.3 The Ribbon and the Climber Sideways

A small eastward displacement $u(r,t)$ of the ribbon obeys the taut-string equation with the tidal term of the rotating frame, Equation (12.6), fixed at the anchor and carrying the counterweight at its upper end.

$$\lambda\, u_{tt} = (T u_r)_r - \lambda\, \kappa(r)\, u + f, \qquad \kappa(r) = \frac{\mu}{r^3} - \omega^2 \tag{12.6}$$

The tidal stiffness κ restores below the geostationary radius and destabilizes above it. Eight hundred linear finite elements stretched toward the anchor, $r_i = R_E + L(\mathrm{e}^{\beta i/N}-1)/(\mathrm{e}^{\beta}-1)$ with $\beta=9$, lumped nodal masses $\lambda_i \ell_i$, element stiffnesses $T(r_{i+1/2})/h_i$, the tidal term $\lambda_i \kappa(r_i)\ell_i$ on the diagonal and the counterweight's mass and tidal stiffness at the top node give a symmetric tridiagonal eigenproblem whose six lowest modes are found by Sturm bisection and inverse iteration. Each mode shape ϕ_k is scaled to a unit peak, so the modal coordinate q_k is that mode's largest deflection in meters. The periods are 127.40, 7.929, 4.061, 2.722, 2.047 and 1.640 h, with modal masses from 2163 t down to 929 t. The climber drives each mode through its guide-roller force in proportion to the mode's shape at its height, as shown in Equation (12.7).

$$M_k\left(\ddot{q}_k + 2\zeta_k \Omega_k \dot{q}_k + \Omega_k^2 q_k\right) = \phi_k(r_c)\, F_{link} \tag{12.7}$$

Six string modes cannot represent the give of the ribbon between the anchor and a climber low on it, so that residual flexibility carries its own degree of freedom, the climber's lateral position u_c, in Equation (12.8).

$$\begin{aligned} m\ddot{u}_c &= -2m\omega v + F_y - F_{link} - m\,\kappa(r_c)\, u_c \\ F_{link} &= k_L w + c_L \dot{w}, \qquad w = u_c - \textstyle\sum_k \phi_k(r_c)\, q_k \end{aligned} \tag{12.8}$$

where $\dot{w}$ includes the rate $\phi_k'(r_c)\, v\, q_k$ at which the climber moves along the modal shapes. The Coriolis force $-2m\omega v$ pushes a climbing climber west and a descending one east, and it vanishes while the climber is held. It is the rotating-frame term that Chapter 11 cancels with a feedforward on its thrusters. The climber has no lateral actuator, so only the timing of its speed changes acts on this push. The flexibility and damping of the link follow Equation (12.9).

$$\begin{aligned} \frac{1}{k_L} &= G(r_c) - \sum_k \frac{\phi_k^2(r_c)}{M_k \Omega_k^2} + \frac{1}{k_a} + \frac{\Lambda^2 F_{on}}{\max(0.02z,\; z-\Lambda F_{on})} \\ c_L &= 2\zeta_s \sqrt{k_L m} + \frac{T(r_c)}{c} \end{aligned} \tag{12.9}$$

Here $\Lambda(r_c) = \int_{R_E}^{r_c} \mathrm{d}r'/T(r')$ is the series flexibility of the ribbon below the climber, and $G(r)$ is the static deflection at r under a unit lateral force there, the diagonal of the inverse stiffness, from which the share of the six modes is removed. The last term is the extra give of the ribbon below the climber while the force F_{on} the climber rides on takes tension off it, which for a uniform string is exactly the change from z/T to $z/(T-F_{on})$. The damping adds the impedance T/c of the ribbon above, which carries away the waves the climber launches upward. The sway reported by the application is the local motion beyond the quasi-static deflection under the loads of the moment, $s = w - (-2m\omega v + F_y)/k_L$.

12.3.4 Air, Wind and Side Load

The crosswind has a single-peaked profile with its maximum at $z_j = 10\,\text{km}$ and first-order gusts, and it loads the climber only, since the ribbon is taken as edge-on to the wind. The side force has a normal-force part that grows with the product of the climbing speed and the wind, the $q\alpha$ load of an ascending vehicle, and a crossflow drag, as shown in Equation (12.10).

$$\begin{aligned} V_w &= \psi(z)\,(V_j + \gamma_k), \qquad \psi(z) = \frac{z}{z_j}\,\mathrm{e}^{1-z/z_j} \\ \gamma_{k+1} &= \alpha_g\,\gamma_k + \sqrt{1-\alpha_g^2}\,\sigma_g n_k \\ F_y &= \tfrac{1}{2}\,\rho(z)\,V_w\big(C_{N\alpha}A_f|v| + C_c A_s|V_w|\big) \end{aligned} \tag{12.10}$$

Here $\alpha_g = \mathrm{e}^{-\Delta t_c/\tau_g}$ with $\tau_g = 20\,\text{s}$, n_k is a standard normal deviate drawn every control period and the profile ψ is zero above $12 z_j$. At the height of the jet the air density is $0.378\,\text{kg/m}^3$.

12.3.5 Heat

The motor and the brake are lumped thermal masses, given in Equation (12.11).

$$\begin{aligned} C_m\frac{\mathrm{d}T_m}{\mathrm{d}t} &= c_{cu}F_{tr}^2 - hA_m(T_m - T_{air}) \\ &\quad - \chi(z)\,\varepsilon\sigma A_m\big(T_m^4 - T_{sink}^4\big) \\ C_b\frac{\mathrm{d}T_b}{\mathrm{d}t} &= |F_b\,v| - hA_b(T_b - T_{air}) \\ &\quad - \varepsilon\sigma A_b\big(T_b^4 - T_{sink}^4\big) \end{aligned} \tag{12.11}$$

Here σ is the Stefan-Boltzmann constant. The forced convection of a cooler rated hA_{50} at 50 m/s at sea level scales as $hA_{50}(\rho/\rho_0)^{0.8}(\max(|v|, 5\,\text{m/s})/50\,\text{m/s})^{0.8}$, the fans supplying the 5 m/s at rest. The motor's radiator is stowed in the air and opens over 2 km around $z_{rad} = 40\,\text{km}$, $\chi = \text{clamp}[(z - z_{rad})/2\,\text{km} + 0.5,\ 0,\ 1]$, while the brake radiates at every height. The air cools at 6.5 K/km to 216.65 K at 11 km and stays there. The copper loss depends on the force and not on the speed, which is what makes a slow climb through the thin air hot.

12.3.6 Tension, Energy Ledger and Instruments

The force the climber rides on comes off the ribbon below it, so the anchor tension is $T_a = T_0 - F_{on}$, with $F_{on} = F_{tr} + F_b$ in motion, mg_{eff} on the clamp and F_{tr} on the platform. Seven ledgers integrated with the states give the energy balance of Equation (12.12).

$$E_{in} - E_{out} - E_{cu} - E_{aux} = \Delta E_{mech} + E_{bk} + E_{dr} + E_{ct} \tag{12.12}$$

The left side is the electrical energy supplied, less the energy returned, the copper loss and the auxiliary load, and the right side is the change of mechanical energy $E_{mech} = \frac{1}{2}mv^2 + m[\Phi(r) - \Phi(R_E)]$ plus the brake heat, the drag work and the kinetic energy absorbed by the clamp and the platform. A further ledger E_{dmp} accumulates what the lateral damping removes.

No loop reads the true state. The controller sees the height by ranging with 0.5 m of noise, the speed through a tachometer with 0.02 m/s of noise plus the bias b_v, the traction force with 0.2 kN of noise, the motor temperature after a 20 s first-order lag, with 0.2 K noise, and the brake temperature after a 5 s lag, with 1.0 K noise, each sampled once a second. A lateral fix of u_c (3 s lag, 1.0 m), an anemometer (2 s, 0.3 m/s), the anchor load cell (2 s, 0.5 kN) and a guide-roller load cell (30 N) are logged for the trends and the export, and no decision reads them. The speed schedule instead takes the mean crosswind V_j and the gust intensity σ_g as a wind profiler would report them.

Table 12.2 Parameters of the Climber and the Ribbon

Symbol	Meaning	Value
adjustable in the model dialog		
c^2	working specific strength	40 MJ/kg
T_0, r_{cw}	anchor tension, counterweight	320 kN, 100 000 km
N_m	lateral modes kept	6
ζ_k, ζ_s	modal, guideway damping	1 %, 1 %
k_a, $T_{a,min}$	anchor stiffness, tension floor	5000 N/m, 64 kN
m_e	climber empty mass	5.0 t
A_f, C_D	frontal area, drag coefficient	12 m^2, 0.80
$C_{N\alpha}$, C_cA_s	normal-force slope, crossflow	2.0 rad^{-1}, 36 m^2
$F_{g,max}$	guide-roller rating	6.00 kN
F_I, τ_F	current-limit force, drive lag	280 kN, 2.0 s
μ_s, μ_k, N_c	traction, sliding, clamp force	0.45, 0.35, 500 kN
c_{cu}, P_{aux}	copper loss, auxiliary load	12 W/kN^2, 40 kW
P_{sup}, $\dot{P}_{sup}$	supply, ramp rate	6.0 MW, 25 %/min
P_{rg}, v_{max}	regeneration, roller speed	2.0 MW, 100 m/s
F_{b0}, T_{fade}	brake capacity, fade onset	250 kN, 650 °C
C_m, hA_m	motor capacity, air cooling	2.0 MJ/K, 10 kW/K
A_m, z_{rad}	radiator area, opens above	260 m^2, 40 km
$T_{m,max}$, $T_{b,max}$	winding and brake limits	150, 600 °C
C_b, hA_b	brake capacity, air cooling	0.80 MJ/K, 4.0 kW/K
A_b	brake radiating area	15 m^2
ε, T_{sink}	emissivity, radiative sink	0.85, 250 K
ρ_0, H	sea-level density, scale height	1.225 kg/m^3, 8.5 km
z_j, τ_g	jet height, gust correlation	10 km, 20 s
fixed in the code		
μ	gravitational parameter	$3.986\,004\,418 \times 10^{14}$ m^3/s^2
ω	sidereal rotation rate	$7.292\,115\,9 \times 10^{-5}$ rad/s
R_E	equatorial radius	6378.137 km
g_0	constant-gravity feedforward	9.806 65 m/s^2
N, β	ribbon elements, stretching	800, 9
v_ε	brake direction smoothing	0.05 m/s
Δt, Δt_c	integration, control period	0.5 s, 1 s

12.3.7 Numerics and Starting State

Table 12.2 gives every parameter. All 42 model parameters can be changed in the application's model dialog, and the constants of the code are listed apart from them. Classical fourth-order Runge-Kutta integrates the thirty states on a 0.5 s step of the shared engine of Section 1.6.1. Its clock runs in minutes here, so the derivatives are written per second and scaled by 60 s/min. The controller and the instruments run every second, the historian logs six rows per simulated minute, and the speed selector spans 0.05 to 120 simulated minutes per wall-clock second. The contact and limit logic runs after each integration step. Every case starts on the quasi-static lateral shape for its Coriolis and mean-wind load F_{ext}, $q_k = \phi_k F_{ext}/(M_k\Omega_k^2)$ and $u_c = \sum_k \phi_k q_k + F_{ext}/k_L$, with the drive holding $mg_{eff} + D$ except on the platform or the clamp, and both temperatures start at 20 °C.

12.3.8 Assumptions

The ribbon's material, the power delivery, the guideway integrated with the ribbon, the anchor platform and the deployment are hypothetical. The model applies standard physical relations to declared inputs, and its plausibility is that of the relations, not of the inputs.

The ribbon is axially rigid, so a change of traction force reaches the anchor at once and the travel of the axial wave is left out. The lateral motion stays in the orbit plane, without out-of-plane librations and without the Moon, the Sun or the Earth's oblateness.

The coupling is one-way. The lateral motion does not feed back on the radial motion, and the radial Coriolis term it would add, $2m\omega\dot{u}_c$, stays below 8.0×10^{-5} of the weight in every case and variant below 1000 km and below 0.97 N in case 5.

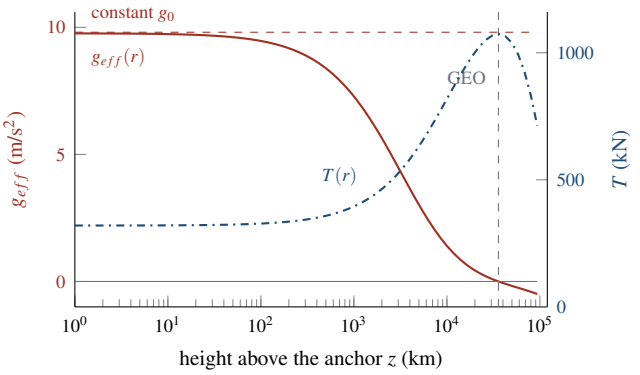


Figure 12.2 Effective gravity (thick solid line, left axis) and ribbon tension (thick dash-dotted line, right axis) along the route at the default inputs. The thin dashed horizontal line is the constant g_0 a naive feedforward would assume, and the dashed vertical line marks the geostationary altitude, 35 786 km, where T peaks at 1073.7 kN and beyond which g_{eff} points outward. The curves end at the counterweight, 93 622 km above the anchor.

Six string modes and one local degree of freedom represent the lateral motion. The local part is drawn with a static shape, and the impedance T/c stands in for the waves the climber launches, which holds while they take longer to come back than the local period.

A case that starts in motion starts on the quasi-static shape for its load. For the 127.4 h mode that is an idealization, since a real ribbon's state would depend on the history of every climber on it.

The motor and the brake are single thermal masses with illustrative coefficients, a forced-convection law, a radiator that opens above 40 km and a brake that fades linearly above 650 °C, and roller slip is a sliding coefficient with no slip dynamics.

The atmosphere is exponential with an 8.5 km scale height, the crosswind has one peak and first-order gusts and acts on the climber only, and the aerodynamic coefficients are not those of any measured vehicle.

12.4 Gravity That Fades and a Mode That Moves

12.4.1 The Weight Along the Route

The effective gravity and the ribbon tension along the whole route are plotted in Figure 12.2. Below 100 km the effective gravity stays within 3.1 % of its anchor value, which is why terrestrial hoists can treat gravity as a constant. It falls to 9.318 m/s^2 at 150 km, 7.283 m/s^2 at 1000 km and 1.399 m/s^2 at 10 000 km, a seventh of g_0, and it changes sign at the geostationary radius. The tension peaks where the effective gravity changes sign, since $\mathrm{d}T/\mathrm{d}r = \lambda g_{eff}$. A climber's weight therefore spans the whole range from the full terrestrial value to a small outward pull, and a feedforward that is right at one end of the route is wrong at the other unless it models the physics.

12.4.2 The Local Mode

Low on the ribbon the retained modes carry little of the flexibility, 0.4 % of G at 10 km and 5.9 % at 150 km, so Equation (12.9) is dominated by the string below the climber. Treating that string as uniform, at the anchor tension less the climber's weight, gives the period and damping ratio of Equation (12.13).

$$T_L \approx 2\pi\sqrt{m\left(\frac{z}{T_0 - m g_{eff}} + \frac{1}{k_a}\right)}, \qquad \zeta_L \approx \zeta_s + \frac{T(r_c)/c}{2\sqrt{k_L m}} \tag{12.13}$$

Table 12.3 Local Mode of the Climber From the Application and From Equation (12.13)

z (km)	m (t)	T_L app (min)	T_L Eq. (min)	ζ_L app	ζ_L Eq.	modal share
10	11	2.381	2.385	0.062	0.063	0.4 %
150	5	5.341	5.486	0.277	0.285	5.9 %
150	11	8.888	9.122	0.212	0.218	5.9 %
150	14	10.738	11.024	0.202	0.207	5.9 %
400	11	13.688	14.646	0.340	0.363	14.8 %
1000	11	19.099	22.425	0.528	0.618	32.1 %

The period grows with the square root of the height and of the mass, and a heavier climber is slower twice over because its own weight also unloads the string it rests on. The damping comes almost entirely from the ribbon above, which absorbs the local motion as a dashpot of coefficient T/c, the characteristic impedance $\sqrt{T\lambda}$ of a string. The impedance changes little with height while the stiffness falls, so the local mode is lightly damped near the anchor and well damped high up. Equation (12.13) is compared with the application's own local mode in Table 12.3. It agrees to within 2.7 % up to 150 km and overestimates the period by 7.0 % at 400 km and 17.4 % at 1000 km, where the retained modes carry 14.8 % and 32.1 % of the static flexibility that the approximation leaves in the local mode.

🕮 **Pause.** Try Exercise 12.3 before reading on.

12.4.3 The Coriolis Load as a Step

A climber leaving a station at speed v adds the lateral load $2m\omega v$, which the local mode takes up as a quasi-static lean of $2m\omega v/k_L$ to the west. The climber's own move is therefore a disturbance that enters at a known time with a known size, and it can be met only through the command. At 150 km the 11 t climber has $k_L = 1.527\,\mathrm{N/m}$, so the 86.6 N of its case 3 cruise at 54.0 m/s would lean it 56.7 m, and the lean grows as the climber rises and the link softens. The acceleration to that speed takes 3.99 min, less than half the 8.9 min period, and to the mode it is close to a step. A 0.3 m/s^2 limit and a 5 mm/s^3 jerk limit set that duration, which is why the planner alone cannot make the start gentle without making it long. The shapers of Section 12.5 instead split the speed change into parts timed against the mode itself.

12.5 Five Layers, One Scan per Second

The controller runs every second in five layers, outermost first, and all of them act on the measurements of Section 12.3. One scan advances the supply ramp and the gust, draws the measurements, re-reads the load sheet while the climber is parked or docked, forms the speed limit and the shaper timing, updates the supervisor, steps the planner and the shaper, computes the speed loop and allocates its demand. Table 12.4 gives the defaults, the ranges and the fixed margins.

12.5.1 The Speed Schedule

With the fixed schedule the speed limit is $v_{lim} = \min(V_{cr}, v_{max})$. With the scheduled one it is also capped at the three speeds of Equation (12.14).

$$
\begin{aligned}
v_P &: \ \left[\hat{m}(g_{eff} + 0.02) + \hat{D}\right] v + c_{cu} F^2 + P_{aux} = 0.95\, P_{av} \\
v_G &= \frac{0.8\, F_{g,max} / (\tfrac{1}{2}\rho \hat{V}) - C_c A_s \hat{V}}{C_{N\alpha} A_f} \\
\hat{V} &= \psi(z)\left(|V_j| + 2.5\sigma_g\right) \\
v_B &: \ \left(F_{hold} - F_{rg}\right) v = \dot{Q}_b \left(T_{b,max} - 80\,\mathrm{K}\right)
\end{aligned}
\tag{12.14}
$$

Table 12.4 Controller Settings, Their Defaults and Their Ranges

Setting	Default	Range
cruise speed V_{cr}	60 m/s	5–100
speed-loop gain $K_{c,v}$	0.10 s^{-1}	0.01–0.50
integral time $\tau_{I,v}$	40 s	5–300
height-trim gain K_x	0.020 s^{-1}	0–0.10
acceleration, jerk a_{max}, j_{max}	0.30 m/s^2, 5 mm/s^3	0.05–1, 1–100
shaper period T_s/T_L	100 %	50–150
cargo on the load sheet	6 t	0–20
gravity feedforward $\hat{g}$	$g_{eff}(r)$	g_0, off
speed schedule	scheduled	fixed
input shaper	off	ZV, ZVD
regeneration, thermal check	on, on	off
traction, guide, power margins	0.9, 0.8, 0.95	fixed
tension margin, gust allowance	8 kN, $2.5\sigma_g$	fixed
trim authority, reference lead	±2 m/s, 20 m	fixed
brake handover, shaper update	10 kN/s, 3 %	fixed

The power speed v_P, with F the bracketed force, applies on the way up. The guide speed v_G is the lowest over seven heights spread across the look-ahead $v^2/(2a_{max}) + v(a_{max}/j_{max} + t_n) + 200\,\text{m}$, which covers braking and the shaper's delay t_n, and it is never below 3 m/s. Here $\psi(z)$ is the wind profile of Equation (12.10). The brake speed v_B applies on the way down, with $F_{hold} = \hat{m} g_{eff} - \hat{D}$, F_{rg} the regeneration available at that speed and $\dot{Q}_b$ the heat the friction brake sheds steadily at 520 °C, taken as the lowest over five heights below the climber. The speeds v_P and v_B are found by bisection between 0.5 m/s and v_{max}.

12.5.2 The Planner and the Shaper

The planner is a time-optimal jerk-limited generator, derived from the one the air taxi of Volume 20, Chapter 3 and the lift-plus-cruise aircraft of Volume 20, Chapter 4 fly with, that keeps $|\dddot{z}_r| \le j_{max}$, $|\ddot{z}_r| \le a_{max}$ and $|\dot{z}_r| \le v_{lim}$, starts braking when the distance left equals the jerk-limited stopping distance, which from speed v at zero acceleration is $v^2/(2a_{max}) + v\,a_{max}/(2j_{max})$ when $v \ge a_{max}^2/j_{max}$ and $v\sqrt{v/j_{max}}$ otherwise, and advances in ten substeps per scan. While it accelerates it looks one substep ahead under the steepest jerk and brakes at once if waiting would carry it more than 0.5 m past its braking point, and a reference moving away from its target with more than 1 m of stopping distance is first halted and then starts a fresh move from rest. Within 0.05 m, 0.05 m/s and $0.1a_{max}$ of the target it hands over to a linear capture law, $\dddot{z}_r = 3\nu[\nu(\nu e/3 - \dot{z}_r) - \ddot{z}_r]$ with $\nu = (4j_{max})^{1/3}$ in SI units, clamped to the jerk and acceleration limits. The shaper convolves this reference with the impulse trains of Equation (12.15).

$$\begin{aligned} \text{ZV: } A &= \frac{[1,\ K]}{1+K}, \quad t = \left[0,\ \frac{\pi}{\omega_d}\right] \\ \text{ZVD: } A &= \frac{[1,\ 2K,\ K^2]}{(1+K)^2}, \quad t = \left[0,\ \frac{\pi}{\omega_d},\ \frac{2\pi}{\omega_d}\right] \\ z_{sh}(t) &= \textstyle\sum_i A_i\, z_r(t - t_i), \qquad K = \mathrm{e}^{-\zeta\pi/\sqrt{1-\zeta^2}} \end{aligned} \tag{12.15}$$

The speed and acceleration references are convolved the same way. The mode (ω_d, ζ) is predicted from the load sheet and the ribbon model at the measured height, Equation (12.9) with the load-sheet mass $\hat{m}$ and $F_{on} = \hat{m} g_{eff}(z_m)$, and its period is multiplied by the adjustable ratio T_s/T_L. For the 11 t climber at 150 km the prediction is 8.888 min with $\zeta = 0.212$, which gives ZV impulses of 0.664 and 0.336 at 0 and 4.548 min and ZVD impulses of 0.441, 0.446 and 0.113 at 0, 4.548 and 9.095 min.

The heavy radiation damping makes the second ZV impulse half the first. The impulses are rebuilt only when the predicted period moves by more than 3 % and not while the planner is braking, and each rebuild moves the stored unshaped trajectory by the amount that keeps z_{sh} continuous, within a 7200 s history. Once the unshaped reference has reached the station the freeze lifts, the tail of the shaped reference is re-timed to the period predicted near the station, and the continuity shift sends the unshaped reference on a short move back to it. While the demand is saturated in the direction of travel, a reference governor keeps the shaped height within 20 m of the climber and the reference speed within 0.2 m/s of it.

12.5.3 The Speed Loop and the Height Trim

The speed loop is the framework's shared PID in velocity form of Section 1.6.2, working in acceleration units, with its derivative term set to zero, as shown in Equation (12.16).

$$\begin{aligned} v_{sp,k} &= v_{sh,k} + \mathrm{clamp}\big(K_x(z_{sh,k} - z_{m,k}),\ \pm 2\,\mathrm{m/s}\big) \\ e_k &= v_{sp,k} - v_{m,k}, \qquad P_k = K_{c,v} e_k \\ S_k &= S_{k-1} + P_k - P_{k-1} \\ b_k &= \hat{g}(z_{m,k}) + a_{sh,k} + \hat{D}_k/\hat{m} \\ c_k &= b_k + S_k + I_{k-1} \\ u_k &= \mathrm{clamp}\big(c_k,\ F_{lo}/\hat{m},\ F_{hi}/\hat{m}\big), \quad F_k = \hat{m}\,u_k \\ I_k &= I_{k-1} + \Big[\frac{K_{c,v}}{\tau_{I,v}}\,e_k + \frac{u_k - c_k}{\tau_{I,v}}\Big]\Delta t_c \end{aligned} \tag{12.16}$$

The bias b_k is the feedforward, made of the assumed gravity $\hat{g}$ (g_{eff}, g_0 or zero), the shaped acceleration and the drag model divided by the load-sheet mass. Its gravity term is the static feedforward of a known force in the sense of Section 1.4.3: it needs only the load sheet and the gravity model, and the integral is left to correct their errors. The other symbols map onto Equations (1.10) to (1.12) as $b_k = u_b$, $c_k = v_k$ and $T_t = \tau_{I,v}$, with back-calculation on the integral only and the clamp on the emitted demand. Nothing limits the rate of the demand beyond the 2 s drive lag. A climber slower than its reference, a positive error, raises the force demand. The limits are $F_{hi} = \min(F_I,\ 0.9\mu_s N_c,\ T_0 - T_{a,min} - 8\,\mathrm{kN})$, reduced to $F_P(v_m)$ while climbing, and $F_{lo} = -[\min(F_I,\ 0.9\mu_s N_c) + F_{b0} f(T_{b,m})]$ while moving, raised to $-F_P(v_m)$ while descending. In MANUAL the operator's demand is applied, the loop tracks it with $I_k = F_{man}/\hat{m} - b_k - S_k$ as in Section 1.6.2, and the return to automatic starts the planner from the measured height and speed without a jump.

12.5.4 Braking Allocation

The force demand goes to the motor whenever it drives the motion or the climber is stopped. When it opposes the motion, regeneration takes what the supply accepts, $\min(|F|, F_R(v_m), F_I)$, the motor hands any larger share to the friction brake at no more than 10 kN/s, and the brake fills in what the motor will deliver short of the demand over the next scan, predicted from the measured drive force through the 2 s lag. In automatic the motor command stays within $\pm\min(F_I,\ 0.9\mu_s N_c)$.

12.5.5 The Supervisor

The supervisor moves the climber through the phases parked, release, go and docked, and through stopping and hold when a move becomes infeasible. Its checks run at once and then every simulated minute. A load is feasible while the load-sheet weight $\hat{m} g_{eff}(z_m)$ stays within $T_0 - T_{a,min} - 8\,\mathrm{kN}$, for the tension, and within $0.9\mu_s N_c$, for the grip, and a refusal names the first limit that fails, in the order tension, grip and heat. With the thermal check on, the motor temperature is marched along the rest of the climb in 30 s steps at the power-limited speed with the thermal model of Equation (12.11), and the climb is infeasible when the forecast peak passes the winding limit less 3 K while moving, or less 10 K before a start. A release ramps the drive to the believed weight $\hat{m}\hat{g}$ over 30 s and opens the

Table 12.5 Case Sequence Along the Route

#	Case, segment and change	Teaching point
1	5 t, anchor to 150 km	a weight that fades
2	15 t, same climb	the limit that binds
3	11 t, 150 to 400 km at 5 min	Coriolis sway on departure
4	11 t to 60 km, 15 m/s jet, gusts	slow down in the wind
5	11 t, 100 m/s across GEO	weightless, then outward
6	11 t, supply 20 % at 6 min	forecast and hold
7	stop at 150 km, sheet 3 t light	shaping a stop
8	11 t, 100 km down, 40 m/s	braking capacity
9	13 t to 150 km in the wind	graded transfer

clamp only once the measured drive force has reached 99 % of it. An infeasible climb stops from where the climber is at the jerk and acceleration limits, clamps, and holds for at least 60 s and until the forecast clears. The climber docks when the shaped reference is within 0.5 m and 0.02 m/s of the station, the planner has captured it and the climber is within 1 m and 0.05 m/s, or when it rests on the platform with the anchor as its destination. Falling toward the anchor faster than the planned stop allows, the planner brakes at up to 3 m/s^2 to protect the platform.

12.5.6 Three Models Kept Apart

Section 12.3 describes the simulation model. No identification runs inside the application, yet the loop's control model follows from Equation (12.3). With an exact feedforward the demand u reaches the speed as an integrator behind the drive lag, $v/u = 1/[s(\tau_F s + 1)]$, and the default $K_{c,v} = 0.1\,\mathrm{s}^{-1}$ puts the crossover near 0.1 rad/s, much faster than the 0.0118 rad/s of an 8.9 min local mode, so the loop tracks the reference that excites the mode rather than damping the mode. The controller's internal models are the load-sheet mass, the assumed gravity, the drag model, the ribbon model at the load-sheet mass for the shaper and the motor model for the forecast. Only the load sheet can be made wrong by a disturbance.

12.6 Cases and What They Measure

Table 12.5 lists the cases and Table 12.6 what they showed. Each case starts from the defaults of Table 12.4 apart from the changes named, and every number below comes from the engine run without its interface at that case's own seed, with times in simulated minutes from the case's start. A change is made after the case is loaded and before Run, so it acts from the first scan, unless the text says it was carried through Reset, which keeps the learner's settings as Section 1.6.4 describes. Each case covers one segment of the route. A climber lifts off when it is 0.5 m above the platform.

12.6.1 A Weight That Fades

The empty 5 t climber of case 1 rests its 48.8 kN weight on the platform until the release has proved the drive, lifts off at 1.775 min and takes the anchor tension from 320 to 271.2 kN. The tension is lowest, 260.3 kN, at 5.01 km, where the drive still accelerates the climber against 9.66 kN of drag. The drag peaks at 9.80 kN at 5.60 km and 56.8 m/s, the power at 3.56 MW at 6.91 km, and above the air the climber cruises on 46.73 kN at 140 km, the weight at an effective gravity of 9.347 m/s^2 with no drag left. It docks at 48.57 min, 1.62 m from the station mark, having drawn 2084 kWh, and its speed stays within 0.46 m/s of the reference. Without the feedforward the release has no weight to ramp to, the climber rests on the platform until the integral has built up the whole weight, lifts off at 3.56 min, falls 3.45 km behind its reference and catches up at 1.05 m/s^2.

Table 12.6 What Each Case Measured

Case	Measured outcome
1, lift-off, cruise	1.775 min on 48.8 kN, 46.73 kN at 140 km
1, drag, power	9.80 kN at 5.60 km, 3.56 MW at 6.91 km
1, dock	48.57 min, 1.62 m off the mark, 2084 kWh
1, no feedforward	lift-off 3.56 min, 3.45 km behind
2, speed limit	36.28, 37.29, 38.08 m/s at 10, 40, 100 km
2, trip, motor	69.9 min, 116.1 °C at 121.4 km
2, 12 and 22 t	forecast 145 °C, tension and traction, stays
3, departure sway	30.84 off, 26.86 jerk, 10.02 m a_{max} 0.1
3, shaped departure	ZV 20.09 m, ZVD 13.17 m
3, after the move	21.36, 2.31, 2.43 m off, ZV, ZVD
4, guide load	fixed 6.94 kN, scheduled 5.42 kN
4, lift-off to 20 km	8.1 min fixed, 16.2 min scheduled
5, $g_{eff} = 0$	14.325 min, 86.7 N to hold at the station
5, constant g_0	false 107.9 kN, overspeed in 2.5 s, 169.1 m/s
6, forecast, hold	147.6 °C at 9.08 min, held 11.98–60.93 min
6, dock, check off	108.98 min at $\leq$ 64.1 °C, off 168.3 °C
7, docked sway	28.84, 6.97, 1.19 m off, ZV, ZVD
7, dock time	24.83, 27.48, 30.73 min
8, fixed 40 m/s	brake 1037 °C, 1421 kWh back, 1438 kWh heat
8, scheduled	518 °C, 2314 kWh back, 72.5 min
8, no regeneration	570 min to the anchor

TRY IT IN THE APP **1 · Unloaded Climb**

Load the scenario and press Run. Watch the drive force on the Forces trend. The empty climber rests on the platform until its drive holds the 48.8 kN weight, lifts off at 1.775 min and, above the air, cruises on 46.73 kN at 140 km. The force it must hold has fallen with height. It docks at 48.57 min.

Tripling the mass in case 2 on the same 6 MW supply limits the speed to 36.28, 37.29 and 38.08 m/s at 10, 40 and 100 km as the weight falls, and the station is reached 69.9 min after lift-off instead of 46.8 min. The anchor tension falls to 165.5 kN and the rollers work at 68.7 % of their traction. The copper loss is nine times the empty climber's, and above 40 km only the radiator removes it, so the motor peaks at 116.1 °C at 121.4 km. On the 0.5 t steps of the load sheet, the largest cargo that leaves the platform is 11.5 t, with a forecast of 134 °C. At 12 t the forecast is 145 °C, above the 140 °C allowed for a start, and at 14 t it is 208 °C. On the same steps the supervisor names heat as the refusing limit from 12 to 15.5 t, the grip of the rollers from 16 to 20 t and the anchor tension from 20.5 t. With 22 t the load-sheet weight of 263.6 kN would take the anchor tension to 56.4 kN, below its floor, and exceed the 225 kN the rollers can grip. Heat, and not power, sets the largest load.

Near the geostationary altitude the weight is almost gone. In case 5 the effective gravity is 0.001 37 m/s^2 at the start, crosses zero 14.325 min in at 35 786 km and is −0.007 88 m/s^2 at the station, where holding the 11 t climber takes 86.7 N pulling inward. From 2 to 40 min the drive delivers between −52.9 and 44.6 N, and the climber draws 34.7 to 44.5 kW, most of it the 40 kW auxiliary load. The Coriolis force at 100 m/s is 160.4 N, the climber sits 66.0 km west of the radial line, and the slowest mode holds its 157.8 km deflection at the counterweight through the case while the 7.93 h mode moves between 2.32 and 1.56 km. The climber docks at 101.80 min. Switched to the constant g_0 at 20 min, 34 km past the geostationary altitude, the feedforward believes in a 107.9 kN weight, the rollers pass their speed rating 2.5 s after the scan that applies it and the speed reaches 169.1 m/s before the integral takes the false weight back. There, a gravity-model error of 0.1 % of g_0, 0.0098 m/s^2, is larger than the whole effective gravity at the station.

Pause. Try Exercise 12.1 before reading on.

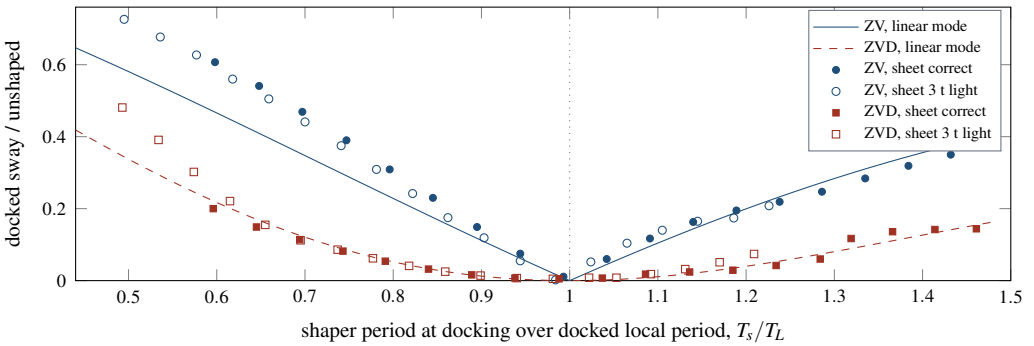


Figure 12.3 Measured sensitivity of a shaped stop to its timing, case 7 run at 19 shaper periods from 60 to 150 % of the prediction, with a correct load sheet (the cargo error set to zero and carried through Reset, since the true mass is fixed when a case starts) and the shipped 3 t light one. Each docked residual is divided by the unshaped one, 18.33 m and 28.84 m, and plotted against the shaper period in force when the climber docks, after the re-timing near the station. The thin solid line (ZV) and the thin dashed line (ZVD) are the residual of the same impulse trains on a linear mode with $\zeta = 0.21$. Circles are ZV runs and squares ZVD runs, filled with a correct sheet and open with the light one.

12.6.2 Sway at a Departure and at a Stop

The 11 t climber of case 3 holds station at 150 km on its drive and leaves for 400 km at 5 min, reaching the 54.0 m/s its supply allows in 3.99 min. The quasi-static lean its Coriolis force demands grows to 78.0 m west within 20 min as the climber rises. Unshaped, the largest sway, 30.84 m at 3.05 min after departure, is a lag rather than an overshoot, because the lean has already reached 50.3 m while the climber has moved only 19.5 m toward it. The climber then overshoots the lean by 21.36 m at 6.77 min. A jerk limit of 2 mm/s^3 barely changes the lag (26.86 m), and an acceleration limit of 0.1 m/s^2, which spreads the start over about a period, cuts it to 10.02 m at the cost of a trip 5.5 min longer. With the shapers the lag falls to 20.09 m (ZV) and 13.17 m (ZVD), 0.651 and 0.427 of the unshaped value, close to the first impulses of 0.664 and 0.441, because until the second impulse arrives the mode sees only the first share of the speed change. What the shapers remove is the ringing after the move. In the 20 min after each shaped acceleration has fallen below 0.01 m/s^2 the largest sway is 2.31 m with ZV and 2.43 m with ZVD, against the 21.36 m unshaped overshoot, and at the 400 km station the unshaped stop leaves 62.58 m ringing while docked, ZV 0.34 m and ZVD 0.07 m. The sway read during a move is this lag, which falls only by the first impulse's share, while the shapers remove nine tenths of the ringing that follows.

🕮 **Pause.** Try Exercise 12.2 before reading on.

Case 7 releases the local mode at a stop, as the Coriolis push of a 40 m/s cruise is removed, with a load sheet 3 t light. Unshaped, the climber docks at 24.83 min with 28.84 m of sway ringing. The impulses freeze when the planner starts braking, at a predicted period of 8.52 min for the 11 t on the sheet. Once the unshaped reference reaches the station they are re-timed to the period predicted there, 8.82 min for ZV at 20.92 min and 147.7 km and 8.78 min for ZVD at 20.22 min and 146.1 km, and the continuity shift sends the reference 89 m and 159 m back to the station. Carried through Reset, ZVD is re-timed at 20.15 min and 146.0 km instead, because a shaper switched on during the cruise first moves the unshaped reference by 6.5 km to keep the shaped one continuous. Both periods remain short of the 10.74 min mode that the 14 t on board gives the docked climber. ZV docks at 27.48 min and leaves 6.97 m, and ZVD docks at 30.73 min and leaves 1.19 m. Each shaper costs part of a period.

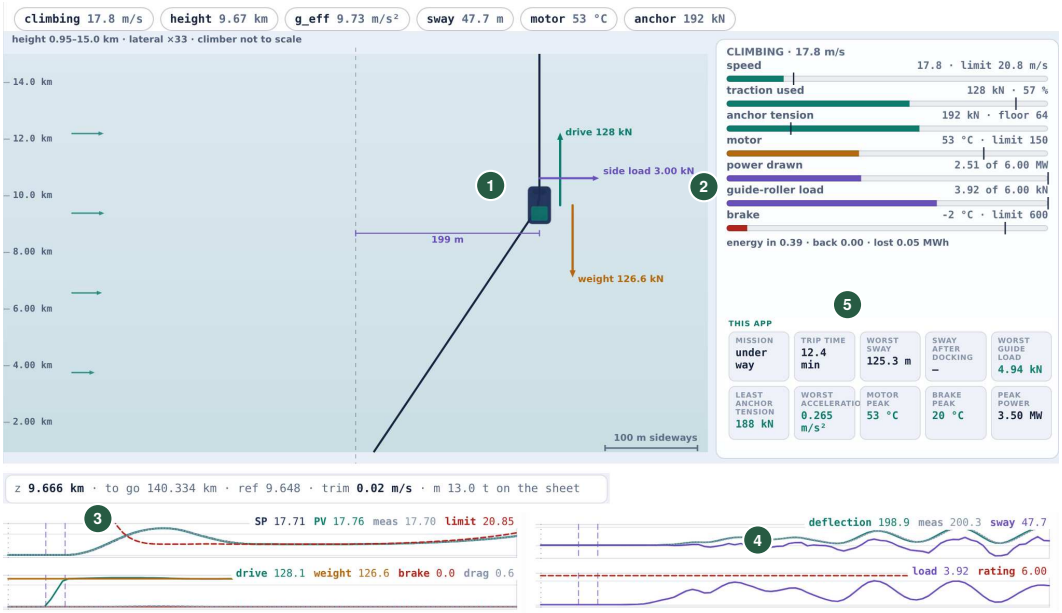


Figure 12.4 The application in the graded transfer, *Challenge, Cargo to the 150 km station*, run with the suggested configuration (scheduled speed limit, ZV shaper and $g_{eff}(r)$ feedforward) and paused at $t = 14.00$ min. The picture is a composite of parts of one screenshot: the Climber view with its plate, the scorecard tiles set into the plate's empty lower part, the station-stop status line and four of the trend strips. The 13 t climber is in the jet at 9.666 km, climbing at 17.76 m/s under a 20.85 m/s limit. In the run at that moment its drive develops 128.0 kN against a 126.6 kN weight and 0.6 kN of drag. The scene draws the height from 0.95 to 15.0 km and the lateral direction at 33 times that scale, and the 3.00 kN side-load arrow and the 199 m eastward deflection at the climber (1) are each read on their own labeled scale. The plate reads 3.92 of 6.00 kN on the guide rollers (2), 192 kN of anchor tension over its 64 kN floor, 57 % of the traction, 2.51 of 6.00 MW drawn, 53 °C at the motor and −2 °C at the brake in the cold air. On the strips the dashed vertical marks are the supervisor's release and departure, at 1.02 and 1.57 min of the run, the speed limit dips ahead of the jet (3), to 10.1 m/s in the run, and rises again, the deflection reads 198.9 m with 47.7 m of local sway (4), and the guide-roller load swings below its rating. The scorecard's worst sway of 125.3 m (5) is mostly the climber lagging a lean that the gusts move faster than its 2.49 min local mode at 8.4 km can follow, while its worst guide load is 4.94 kN.

A sweep of the shaper period is carried out in Figure 12.3 over 76 runs, all of which dock. Plotted against the ratio of the shaper period in force at docking to the docked local period, the two load sheets fall on one curve for each shaper, and the residual of the same impulses on a linear mode describes them with a root-mean-square difference of 0.053 of the unshaped residual. The notches of both shapers sit at 0.98 to 0.99. With a correct sheet ZV leaves 0.21 m at 0.993, where the unmodified prediction re-timed near the station, 8.82 min, is within 0.7 % of the docked 8.888 min, and with the light sheet, retimed to 120 % of the prediction, it leaves 0.06 m at 0.984. The period that matters is therefore the one in force for the last impulses, and the 8.52 min frozen at the start of braking would place the notches near 0.95. The residual stays below a tenth of the unshaped value between the samples at 0.74 and 1.21 with ZVD, and only between 0.94 and 1.02 with ZV. The shipped case sits at 0.822 for ZV and 0.818 for ZVD, where they leave 0.242 and 0.041 of the unshaped residual.

Table 12.7 Transfer Configurations Including Twenty Docked Minutes. Result Names the Failed Parts, Guide Is the Worst Guide-Roller Load and Docked the Worst Sway While Docked

Configuration	Result	Guide (kN)	Docked (m)	Dock (min)
shipped[a]	guide, sway	8.15	27.47	60.97
scheduled only	sway	5.10	27.51	69.72
ZV only	guide	8.12	0.22	63.98
g_{eff} only	guide, sway	8.15	27.42	60.97
scheduled, g_{eff}	sway	5.10	27.47	69.93
ZV, g_{eff}	guide	8.12	0.24	64.20
scheduled, ZV, g_0	passes	4.94	0.36	75.10
suggested[b]	passes	4.94	0.36	75.07
suggested with ZVD	passes	4.87	0.10	79.62
suggested, no feedforward	acceleration	4.73	0.27	75.43

[a] fixed 60 m/s, unshaped, constant g_0 [b] scheduled, ZV, $g_{eff}(r)$

12.6.3 Wind, Power and Brakes

In the crosswind of case 4 the fixed schedule meets the jet at 50.2 m/s, 5.17 km up in an 11.7 m/s wind, where the speed-dependent part of the side load is 4.70 kN against 1.64 kN of crossflow drag, and the guide rollers see 6.94 kN against their 6.00 kN rating, an overload the scorecard records. Scheduled, the limit plans to 80 % of the rating with 2.5 gust intensities in hand, the climber slows to 10.1 m/s at 6.0 km and the load peaks at 5.42 kN. The price is time, 16.2 min from lift-off to 20 km against 8.1 min. On seven other gust seeds the scheduled peak ranges from 4.26 to 6.53 kN, past the rating on two of them, and the fixed one from 7.28 to 9.10 kN, so the gust allowance makes an overload rare rather than impossible. Hurrying through the windy layer is the wrong instinct, because 74 % of the side load at the fixed schedule's peak grows with the climbing speed.

> **TRY IT IN THE APP** **4 · Wind in the Atmospheric Segment**
>
> Run the scenario with the scheduled speed and watch the climber slow as it nears the jet, to 10.1 m/s at 6.0 km, while the guide-roller load peaks at 5.42 kN. Press Reset, set the speed schedule to Fixed and run again. The load reaches 6.94 kN, past its 6.00 kN rating, and the climber is 20 km up 8.1 min after lift-off instead of 16.2 min.

Six minutes into case 6 the supply ramps to 20 % over 3.2 min, which leaves the 11 t climber 8.97 m/s. At that speed the motor would spend about 49 min between the air that cools it and the 40 km where its radiator opens. Before the ramp has finished, at the check at 9.08 min, 13.4 km up, the forecast reaches 147.6 °C, past the 147 °C at which a moving climber is stopped. The supervisor stops, holds on the clamp from 11.98 to 60.93 min at 13.9 km, where the motor carries no current and cools while the forecast at the reduced supply reads 168 to 173 °C, and resumes once the supply has returned at 60 min, docking at 108.98 min with the motor never above 64.1 °C. With the check off the climber carries on and the motor reaches 168.3 °C at 57.34 min, 39.6 km up, a recorded over-temperature within 0.3 K of the 168.0 °C forecast at 10.10 min. On six noise seeds the stop falls at the same check and the peak with the check off spans 167.9 to 168.3 °C.

Going down in case 8, the climber's weight must be held back all the way, and at the fixed 40 m/s that is about 4 MW of braking. The motor returns 1421 kWh to the supply, and the friction brake takes 1438 kWh, passes its 600 °C limit 7.79 min in and peaks at 1037 °C. Scheduled, the descent is held to the speed that regeneration and the brake's cooling at 520 °C can absorb, 23.1 m/s on average between 60 and 90 km, and the brake peaks at 518 °C while 2314 kWh return to the supply and 448 kWh become brake heat, in a trip of 72.5 min instead of 45.5 min. Without regeneration the schedule allows 2.7 m/s and the climber reaches the anchor after 570 min.

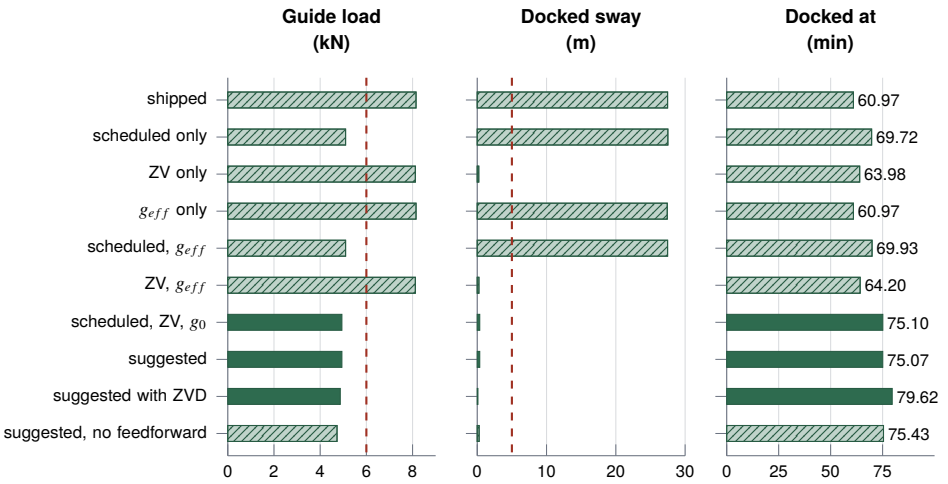


Figure 12.5 Table 12.7 redrawn: the graded transfer in ten configurations. Solid bars pass, hatched bars fail, and the dashed lines are the 6 kN guide-load and 5 m docked-sway limits. Notice that each failing configuration crosses one dashed line or the other, the last row failing on acceleration instead, and that every passing one docks later than any that fails on guide load or sway.

> ✦ **DID YOU KNOW?** **Slower Down, More Energy Back**
>
> From the simulator: descending 100 km at a fixed 40 m/s, the friction brake peaks at 1037 °C and 1421 kWh return to the supply. Held to the scheduled speed, the brake peaks at 518 °C and 2314 kWh return, in a trip of 72.5 min (case 8 of Table 12.6).

12.6.4 The Graded Transfer

The transfer carries 8 t of cargo from the anchor to the 150 km station through the 15 m/s jet with 2 m/s gusts. It passes only if the climber docks within 2 m of the mark and stays 20 min, the guide load stays within 6 kN, the docked sway within 5 m, the anchor tension above 64 kN, the acceleration below 0.5 m/s^2, the motor below 150 °C and the brake below 600 °C, with no slip, no overspeed, no excess of the supply and a closed ledger, and every part is scored on its worst moment. A changed model parameter or disturbance voids the attempt, and the crediting otherwise follows Section 1.6.4. Table 12.7 lists the configurations measured. Figure 12.5 draws the same table as bars against the two limits that most configurations miss.

As shipped, at a fixed 60 m/s, unshaped and with the constant g_0, the climber docks at 60.97 min, but the guide rollers see 8.15 kN at 6.13 km, 2.15 kN over their rating, and 27.47 m of sway rings while it is docked, 22.47 m over its limit. The schedule alone removes the overload and ZV alone removes the sway, and each leaves the other failure in place. Together they pass. The suggested configuration, scheduled with ZV and the $g_{eff}(r)$ feedforward, keeps the guide load to 4.94 kN, 1.06 kN inside the rating, the anchor tension above 188.4 kN, the acceleration below 0.265 m/s^2 and the motor below 93.5 °C, and docks 0.742 m from the mark at 75.07 min with 0.36 m of sway, 14.1 min later than the shipped run. Applied before Run or carried through Reset, the same settings give the same trajectory and result. The constant g_0 in its place still passes, docking 0.353 m from the mark. These errors lie inside the 1 m window on the measured height, read with 0.5 m of noise, within which the supervisor docks, so they reflect that window and not the feedforward. Below 150 km the constant g_0 is at most 6.35 kN wrong for the 13 t climber, and the integral carries it. Removing the feedforward altogether fails the acceleration limit at 0.542 m/s^2. ZVD in place of ZV passes with 0.10 m of docked sway and arrives 4.55 min later. The gusts follow the case's own seed, so every

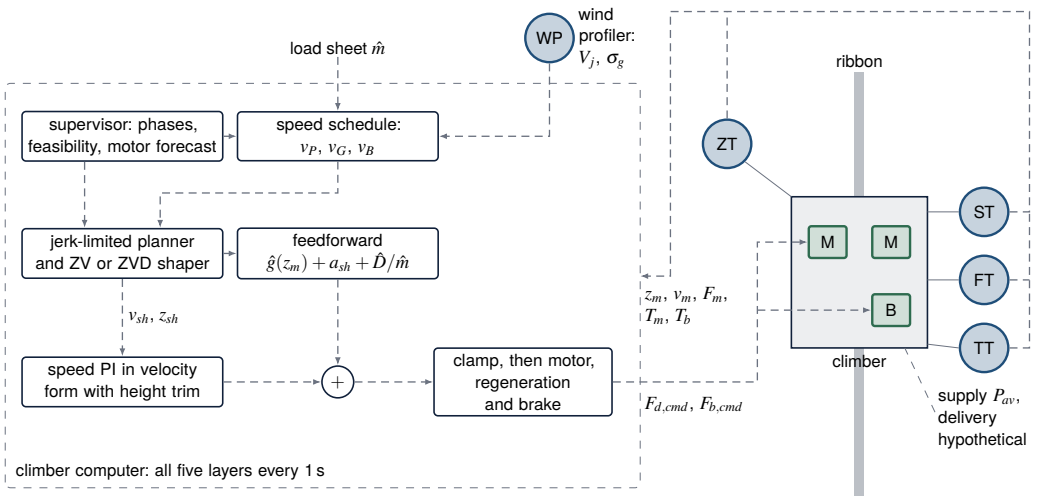


Figure 12.6 The five layers of Section 12.5 on the hardware a climber would carry, which no one has built. Sensors of the kinds flown on tethers and used on drives report height (ZT), roller speed (ST), traction force (FT) and the motor and brake temperatures (TT), and a wind profiler (WP) reports the jet to the schedule. One computer runs the supervisor, the schedule, the planner with its shaper, the feedforward and the speed loop, and splits the clamped demand between the roller motors (M) and the friction brake (B). Dashed gray arrows are signals. Notice that the feedforward block needs only the load sheet, its gravity and drag models at the measured height and the planner's acceleration, while the speed loop corrects whatever they get wrong.

attempt meets the same wind. On seven other seeds the suggested configuration passes six times and on the seventh the guide load reaches 7.02 kN, while the shipped one fails the guide load and the sway on all seven. The feedforward that the transfer barely needs is the one that case 5 cannot do without.

12.6.5 Convergence

The application's 38 checks pass, and they are the evidence for the numerical side of the claim. One of them runs the planner over 360 moves from 10 m to 20 km, from rest and at 9 m/s toward or away from the target, at three sets of limits, and requires every move to capture within 4 h. Halving the 0.5 s step leaves the transfer docking on the same 1 s scan and leaves its worst guide load, docked sway and motor peak unchanged to the digits reported here. Doubling the ribbon grid to 1600 elements moves the six periods by 0.0028 to 0.0346 %, and keeping eight modes instead of six moves the worst sway of case 7 by 0.47 %. The ledger of Equation (12.12) closes to 3.8×10^{-10} of the electrical energy through it on the scheduled descent, 4.5×10^{-10} on the fixed one and 4.8×10^{-11} or better on the unloaded climb, the power restriction and the transfer. Without regeneration, when little electrical energy passes, the residual is 1.2×10^{-5} of it. A Coriolis step at 10 000 km drives modes 2 to 4 to twice their static share $\phi_k \Delta F / (M_k \Omega_k^2)$ within 2.4 %, and a tachometer reading 0.5 m/s fast leaves the case 5 cruise 24.97 m behind its height reference, the $0.5/K_x = 25$ m at which the trim cancels the bias. The transfer as it runs is shown in Figure 12.4.

12.7 Technology in Practice

No space elevator climber has been built, so its hardware can only be borrowed from tethers that have flown and from drives that work on the ground. Figure 12.6 places the five layers of Section 12.5 on such devices.

What Measures It

Flown tether systems measured what this chapter's climber needs. A deployer flown in 1993 and 1994 counted the turns of its tether with light-emitting diodes and carried a tensiometer and a temperature sensor on its brake, and the payload at the far end carried a three-axis tensiometer and a three-axis accelerometer [17]. These are the length, speed, force and temperature readings of Section 12.3, where the height is ranged with 0.5 m of noise and the speed is read by a tachometer, each once a second.

> **TECHNOLOGY Sensor: Counting What Passes**
>
> A flown tether deployer measured its tether by counting. Two light-emitting diodes counted the turns of tether leaving a fixed spool, and a third detected when the spool was almost empty. To give the deployed length and its rate, the turns had to be mapped and converted into length [17]. An optical encoder on a shaft counts the same way, with a slotted wheel that chops a light beam into a train of pulses [18]. A count of this kind gives position and speed directly, but only of the surface it touches and only as well as the map from counts to meters. In the model the speed reading carries noise and the adjustable bias b_v of Table 12.1, which the height trim cancels at a standing offset.

What Moves It

The same deployer controlled its tether with a friction brake: a stepper motor wrapped the tether around a brake post or unwrapped it to change the tension and with it the deployment speed, the friction growing with the contact area [17]. A climber must also push, and the 1999 workshop judged that traction wheels would be slow and would wear the vehicle and the structure [15]. The model gives its rollers a current limit of 280 kN, a grip of 225 kN and a drive lag of 2 s, and its brake a fade above 650 °C.

> **TECHNOLOGY Final Element: A Motor That Brakes as a Generator**
>
> A load lowered by an electric hoist does work on the hoist. A friction brake turns that energy into heat, while regenerative braking switches the motor into a generator and sends the energy back to a battery or the grid [18]. In an alternating-current drive this takes extra power transistors that invert the drive's internal direct voltage back to the line, which makes the drive more expensive and potentially more prone to faults, a cost repaid where the recovered energy is significant. Every electronic braking method depends on the drive working, and where the motor itself can brake, a separate mechanical brake may not be needed [18]. The climber keeps both: regeneration up to the supply's acceptance P_{rg} and a friction brake that fades when hot.

Where the Controller Runs

A terrestrial speed drive closes its own loop on a tachometer and so becomes the secondary controller of a cascade, taking its speed setpoint from the process controller [18]. The flown deployer ran its control logic in its own electronics box and followed a profile computed before the mission [17]. The parts of the handbook read for this section give no execution period for that logic. The application runs all five layers on one computer every 1 s: the supervisor, the schedule, the planner with its shaper, and the speed loop whose bias term carries the gravity feedforward.

> **IN PRACTICE Pay Out When the Tension Is High**
>
> Tethers flown in orbit left rules of practice. The field's handbook states that tension laws can control both the swing of a tethered system and the oscillations of its tether. A swing in the orbit plane is damped by paying out tether when the tension is greater than usual and retrieving it at other times, which absorbs energy from the swing. Because that swing causes large variations in tension through the Coriolis effect, such maneuvers damp it quickly [17]. The climber has no reel and no lateral actuator, so in this chapter only the timing of its speed changes acts on its swing.

What Is Modernizing It

Three developments bear on the climber. The first is power delivered by light. A 2005 assessment took laser power beamed from a ground station to the climber's electric motors as its baseline, demonstrated on the ground but not for a laser that tracks a climber to 100 000 km [10]. A NASA test of a high-intensity laser receiver drew 13.6 W/cm^2 of electrical power from a single photovoltaic cell at a conversion efficiency of 24 percent [19]. In the model this supply is the declared P_{sup} of 6 MW. The second is competition: a NASA prize grant funded tether strength and climber contests meant to advance robotic climbers and beamed power [10]. The third is simulation. A NASA program written for tethered satellite missions was extended to elevator-sized tethers to study deployment, climber dynamics, atmospheric effects and waves induced to avoid objects [10].

12.8 Limitations

The largest limitation is the concept. The ribbon's strength, the power delivery, the guideway, the anchor platform and the deployment are hypothetical, and the dimensions of Section 12.3 follow from declared inputs rather than from a design. The application shows that its equations converge and that its reduced-order behavior is plausible. It does not show that an Earth space elevator can be built, and its numbers are not the numbers of one.

> ⚠ **OPEN CHALLENGE** **A Ribbon No One Can Make Yet**
>
> The most critical technology for an Earth space elevator is a carbon nanotube reinforced composite with a strength in the 100 GPa range. Stresses in the ribbon have been calculated at 60 to 80 GPa. Single nanotubes have been reported above 150 GPa, but making a fiber of that strength from them had been attempted without success, which in a 2005 assessment put the whole Earth-based system at the second of nine technology readiness levels [10]. Progress would be a fiber, and then a ribbon, that keeps that strength after fabrication, splicing and the coatings it needs along its length.

The ribbon is axially rigid and moves laterally in the orbit plane only, the lateral motion does not feed back on the radial, the local mode is drawn with a static shape, and its radiation damping T/c holds only while the waves it launches return more slowly than its period. Cases that start in motion start on the quasi-static shape, an idealization for the 127.4 h mode. The thermal, aerodynamic and structural coefficients are illustrative, and the limits and margins are teaching values. No decision reads the lateral fix, the anemometer or the guide-load measurement, so the lateral dynamics are handled by the schedule and the shaper alone, with no lateral feedback.

The scorecard's worst sway is taken against the quasi-static lean of the moment. In gusts it is dominated by the lean moving faster than the local mode, since the first 14 min of the suggested transfer reach 125.3 m with the 2 m/s gusts and 13.9 m with the gust intensity set to zero, which also removes the schedule's gust allowance, while the worst guide load moves only from 4.85 to 4.94 kN, and on a departure it records the lag rather than the ringing that shaping removes.

> ⚠ **OPEN CHALLENGE** **Ribbon Control Is Still on Paper**
>
> A built elevator would need control systems that hold the ribbon in its orbital slot and govern its tension, induced waves, climber dynamics and atmospheric effects. A climbing climber changes the ribbon's angular momentum, and if the ribbon cannot absorb it, climbers may need thrusters of their own. In 2005 ribbon control was only at an analytical stage, studied with a simulation program built for tethered satellite missions [10]. Progress would be such control demonstrated on a long tether, with the climbers' own speed commands among its inputs.

12.9 Conclusion

The space elevator climber of this chapter is a plant whose weight fades to nothing and reverses along the route, and whose structure answers every change of speed with a slow sideways swing.

The effective gravity falls from 9.764 m/s^2 at the anchor to zero 35 786 km up, where a constant-g_0 feedforward believes in 107.9 kN that is not there and drives an 11 t climber to 169.1 m/s. The climber's local mode, its own mass on the string below it with the ribbon above as the dashpot T/c, is approximated to within 2.7 % up to 150 km, and a departure excites it through 86.6 N of Coriolis force, leaving 21.36 m of ringing unshaped and 2.31 m with ZV. Swept over a stop, the shaped residual follows the linear curve with a root-mean-square difference of 0.053. The schedule cuts a 6.94 kN side load to 5.42 kN and a 1037 °C brake to 518 °C, and the supervisor holds for 48.95 min rather than let the motor reach 168.3 °C. The ribbon's strength and the power delivery remain hypothetical, and the model is planar, axially rigid and coupled one way. A fuller model would add out-of-plane motion, axial waves, several climbers and a lateral estimator fed by the measurements the application already logs. The simulator turns a structure that may never be built into a working example of what feedforward, scheduling and shaping each carry when the load, the structure and the limits all move with the route.

KEY POINTS

- The weight a climber's drive must hold falls with height and reverses past the geostationary radius, so a feedforward right at one end of the route is wrong at the other unless it models the physics.
- Every change of speed changes the Coriolis push, and a departure shorter than half the local period is close to a step for that mode.
- Shapers remove the ringing after a move, 21.36 m unshaped against 2.31 m with ZV, but not the lag during it.
- The schedule alone removes the transfer's guide overload and ZV alone its docked sway. Together they pass.

Where else this applies. Volume 7, Chapter 12 times the same ZV and ZVD impulses against a swinging crane load, and Volume 20, Chapter 3 feeds a load sheet forward on another vehicle whose load changes along the route.

References

[1] S. Kaczmarczyk and W. Ostachowicz, "Transient vibration phenomena in deep mine hoisting cables. Part 1: Mathematical model," *Journal of Sound and Vibration*, vol. 262, no. 2, pp. 219–244, 2003.

[2] O. J. M. Smith, "Posicast control of damped oscillatory systems," *Proceedings of the IRE*, vol. 45, no. 9, pp. 1249–1255, 1957.

[3] N. C. Singer and W. P. Seering, "Preshaping command inputs to reduce system vibration," *Journal of Dynamic Systems, Measurement, and Control*, vol. 112, no. 1, pp. 76–82, 1990.

[4] W. Singhose, "Command shaping for flexible systems: A review of the first 50 years," *International Journal of Precision Engineering and Manufacturing*, vol. 10, no. 4, pp. 153–168, 2009.

[5] P. Lambrechts, M. Boerlage, and M. Steinbuch, "Trajectory planning and feedforward design for electromechanical motion systems," *Control Engineering Practice*, vol. 13, no. 2, pp. 145–157, 2005.

[6] J. D. Isaacs, A. C. Vine, H. Bradner, and G. E. Bachus, "Satellite elongation into a true "sky-hook"," *Science*, vol. 151, no. 3711, pp. 682–683, 1966.

[7] J. Pearson, "The orbital tower: A spacecraft launcher using the Earth's rotational energy," *Acta Astronautica*, vol. 2, no. 9–10, pp. 785–799, 1975.

[8] B. C. Edwards, "Design and deployment of a space elevator," *Acta Astronautica*, vol. 47, no. 10, pp. 735–744, 2000.

[9] S. S. Cohen and A. K. Misra, "The effect of climber transit on the space elevator dynamics," *Acta Astronautica*, vol. 64, no. 5–6, pp. 538–553, 2009.

[10] D. V. Smitherman, Jr., "Critical technologies for the development of future space elevator systems," in *56th International Astronautical Congress*, 2005, paper IAC-05-D4.2.04; NASA Marshall Space Flight Center, NTRS 20060000015.

[11] N. M. Pugno, "On the strength of the carbon nanotube-based space elevator cable: from nanomechanics to megamechanics," *Journal of Physics: Condensed Matter*, vol. 18, no. 33, pp. S1971–S1990, 2006.

[12] S. S. Cohen and A. K. Misra, "Elastic oscillations of the space elevator ribbon," *Journal of Guidance, Control, and Dynamics*, vol. 30, no. 6, pp. 1711–1717, 2007.

[13] P. Williams and W. Ockels, "Climber motion optimization for the tethered space elevator," *Acta Astronautica*, vol. 66, no. 9–10, pp. 1458–1467, 2010.

[14] P. K. Aravind, "The physics of the space elevator," *American Journal of Physics*, vol. 75, no. 2, pp. 125–130, 2007.

[15] D. V. Smitherman, Jr., "Space elevators: Building a permanent bridge for space exploration and economic development," in *AIAA Space 2000 Conference and Exposition*, 2000, aIAA Paper 2000-5294; NASA Marshall Space Flight Center preprint, NTRS 20000105202.

[16] M. P. Cartmell and D. J. McKenzie, "A review of space tether research," *Progress in Aerospace Sciences*, vol. 44, no. 1, pp. 1–21, 2008.

[17] "Tethers in space handbook," Smithsonian Astrophysical Observatory for NASA Marshall Space Flight Center, NASA Contractor Report NASA/CR-97-206807, 1997, nTRS 19980018321.

[18] T. R. Kuphaldt, *Lessons in Industrial Instrumentation*, version 2.33 ed. Open textbook, Creative Commons Attribution 4.0 license, ibiblio.org/kuphaldt/socratic/sinst, 2024.

[19] D. E. Raible, D. Dinca, and T. H. Nayfeh, "Optical frequency optimization of a high intensity laser power beaming system utilizing VMJ photovoltaic cells," NASA Glenn Research Center, Cleveland, OH, NASA Technical Memorandum NASA/TM-2012-217256, 2012, nTRS 20120007096.

12.10 Exercises

12.1 ○ Concept check · 2 min

In case 5 the feedforward is switched from $g_{eff}(r)$ to the constant g_0 at 20 min, when the 11 t climber is 34 km past the geostationary altitude. What happens next?

(a) Little: the effective gravity there is tiny, so the integral absorbs a tiny error unseen

(b) The climber falls back inward, because the bias no longer holds up any weight

(c) The demand saturates on its lower limit and the supervisor holds the climber on the clamp

(d) The bias asks for a 107.9 kN weight that is not there and throws the climber outward

12.2 ○ Concept check · 2 min

In case 3 the ZV shaper lowers the worst sway of the departure only from 30.84 m to 20.09 m, yet it lowers the ringing after the acceleration from 21.36 m to 2.31 m. Why does it do so little during the move?

(a) Until the second impulse arrives, the mode sees only the first impulse's share of the speed change

(b) The shaper is timed for the wrong period, because the load sheet of case 3 understates the cargo

(c) The planner's jerk limit overrides the shaper during the acceleration and restores the unshaped start

(d) The scorecard measures sway from the radial line, so the growing lean itself is counted as sway

12.3 ○ Concept check · 1 min

Table 12.3 gives a damping ratio of 0.062 for the local mode at 10 km and 0.528 at 1000 km. Why is the mode so much better damped high up?

(a) The guideway damping ζ_s rises with height as the motor's radiator opens

(b) The impedance T/c of the ribbon above changes little while the stiffness k_L falls

(c) The six retained string modes lend the local mode their 1 % damping

(d) The Coriolis force grows with height and acts as a damper on the sideways motion

12.4 ▭ Theory and calculation · 6 min

Use Equation (12.1) with the constants of Table 12.2.

(a) Compute the effective gravity at the anchor and at the 150 km station, and by how many percent the constant g_0 overstates each. *Checkpoint:* 9.764 m/s^2 and 9.318 m/s^2, high by 0.43 % and 5.24 %.

(b) Compute the geostationary radius and its height above the anchor. *Checkpoint:* 42 164 km, 35 786 km up.

(c) The graded transfer carries a 13 t climber to 150 km. By how much does a constant-g_0 feedforward overstate its weight there, and which part of the speed loop carries the error? *Checkpoint:* 6.35 kN, carried by the integral.

12.5 Theory and calculation · 6 min

The 11 t climber holds station at 150 km with $T_0 = 320\,\mathrm{kN}$, $k_a = 5000\,\mathrm{N/m}$, $\zeta_s = 1\,\%$ and $c = 6325\,\mathrm{m/s}$. The ribbon tension at the station is 331.7 kN.

(a) Compute the link stiffness k_L of the uniform-string approximation and the period T_L of Equation (12.13). *Checkpoint:* $k_L = 1.450\,\mathrm{N/m}$, $T_L = 9.12\,\mathrm{min}$.

(b) Compute the damping ratio ζ_L of Equation (12.13) with that k_L, and compare both results with the application's 8.888 min and 0.212. *Checkpoint:* $\zeta_L = 0.218$, and the period is 2.6 % long.

(c) The climber leaves at 54.0 m/s. Compute the Coriolis push and the quasi-static lean it demands with the application's $k_L = 1.527\,\mathrm{N/m}$. *Checkpoint:* 86.6 N and 56.7 m.

12.6 Theory and calculation · 6 min

Design the shapers of Equation (12.15) for the local mode of the previous exercise, with an undamped period of 8.888 min and $\zeta = 0.212$.

(a) Compute K, the two ZV amplitudes and the time of the second impulse. *Checkpoint:* $K = 0.506$, then 0.664 and 0.336, the second at 4.548 min.

(b) Compute the three ZVD amplitudes and their times. *Checkpoint:* 0.441, 0.446 and 0.113 at 0, 4.548 and 9.095 min.

(c) The unshaped departure of case 3 lags its lean by 30.84 m. Predict the lag with each shaper from the share of the move that the first impulse carries, and compare with the measured 20.09 and 13.17 m. *Checkpoint:* About 20.5 and 13.6 m.

12.7 App challenge · 8 min

Load scenario 1, Unloaded climb, at its default seed, with every setting as loaded.

(a) Run until the run stops by itself, 10 min after docking. From the exported CSV, read `drive_force_kN` on the first row with `alt_km` at or above 140, and read the Worst acceleration tile. Compare the drive force with mg_{eff} at that height. *Checkpoint:* 46.7 kN, equal to 5000×9.347, and 0.311 m/s^2.

(b) Press Reset, set Gravity feedforward to off before the departure at 1 min, and run until the climber is 10 km up. Read the time of lift-off from the height trend and the Worst acceleration tile, and compare both with part (a). *Checkpoint:* Lift-off near 3.6 min against 1.8 min, and 1.048 m/s^2.

Accept 0.1 kN on the force, 0.2 min on a lift-off time and 0.005 m/s^2 on an acceleration.

12.8 App challenge · 8 min

Load scenario 3, Acceleration-induced sway, at its default seed. Each run goes to 15 min, 10 min after the climber sets off. Read the Worst sway tile.

(a) Run as loaded. *Checkpoint:* 30.8 m.

(b) Press Reset, set Jerk limit to 2 mm/s^3 before the departure at 5 min, and run again. *Checkpoint:* 26.9 m.

(c) Reload the scenario, set Input shaper to ZV before pressing Run, and run. Then reload again and repeat with ZVD. Divide each result by part (a). *Checkpoint:* 20.1 m and 13.2 m, ratios 0.65 and 0.43.

Accept 0.2 m on each tile.

12.9 App challenge · 9 min

Load the challenge, Cargo to the 150 km station, at its default seed. Each run stops by itself 20 min after docking. Read the Worst guide load, Sway after docking and Mission tiles, and the verdict.

(a) Run as loaded (fixed schedule, shaper off, constant g_0). *Checkpoint:* 8.15 kN, 27.5 m, docked at 61.0 min, failed.

(b) Press Reset, set Speed schedule to Scheduled and run. Then press Reset, set Speed schedule back to Fixed and Input shaper to ZV, and run again. *Checkpoint:* Scheduled: 5.10 kN, 27.5 m. ZV: 8.12 kN, 0.2 m. Both fail.

(c) Press Reset, set Scheduled, ZV and Gravity feedforward $g_{eff}(r)$, and run. Read also the docking error, column `metric_stop_error_m` of the exported CSV. *Checkpoint:* Passes: 4.94 kN, 0.4 m, docked at 75.1 min, 0.74 m from the mark.

Accept 0.02 kN on a guide load, 0.1 m on a sway and 0.1 min on a time.

12.10 Application area · 4 min

Before every start the supervisor checks that the load-sheet weight $\hat{m}g_{eff}$ stays within $T_0 - T_{a,min} - 8\,\mathrm{kN}$ for the anchor tension and within $0.9\mu_s N_c$ for the grip of the rollers. The empty climber is 5 t, and $g_{eff} = 9.764\,\mathrm{m/s^2}$ at the anchor.

(a) Compute the largest weight each rule allows and the cargo it corresponds to. *Checkpoint:* Tension 248 kN, 20.4 t of cargo, grip 202.5 kN, 15.7 t of cargo.

(b) Section 12.6.1 reports refusals for heat from 12 to 15.5 t, grip from 16 to 20 t and tension from 20.5 t. Which limit sets the largest cargo, and why is it not the power? *Checkpoint:* Heat, from 12 t, so 11.5 t is the largest that leaves.

12.11 Application area · 4 min

Case 8 brings the 11 t climber down 100 km to the anchor.

(a) Estimate the braking power at the fixed 40 m/s near 100 km, where $g_{eff} = 9.464\,\mathrm{m/s^2}$, and compare it with the 2 MW the supply accepts. *Checkpoint:* About 4.2 MW, roughly twice what regeneration may return.

(b) The potential energy released, $m[\Phi(R_E + 100\,\mathrm{km}) - \Phi(R_E)]$, is about 2937 kWh. What share returns to the supply on the fixed and on the scheduled descent, and what does the schedule cost? *Checkpoint:* 48 % and 79 %, and 27 min more.

12.12 Review the agent · 5 min

An AI assistant reviews the departure of case 3 and writes: “The 30.8 m sway is a disturbance that the speed loop rejects too slowly. Raise the proportional gain $K_{c,v}$ from 0.10 to 0.30 s^{-1} so the loop holds the climber against the Coriolis push. The worst sway should fall by about a third.” Find the flaw, and say how you would check the claim in the application.